

# The Effects of Additional Two Bendings on Manufacturing Thin-walled Tube made of AZ31 Magnesium Alloy Fabricated by New Compound Extrusion

lin xing Li (✉ [1570508019@qq.com](mailto:1570508019@qq.com))

Chongqing University of Technology

HongJun Hu

Chongqing University of Technology, Chongqing, China

Gang Hu

Chongqing University of Technology, Chongqing, China

Ou Zhang

Chongqing University of Technology, Chongqing, China

---

## Research Article

**Keywords:** Magnesium Alloy, FEM, Grains refinement, Dynamic recrystallization

**Posted Date:** April 8th, 2021

**DOI:** <https://doi.org/10.21203/rs.3.rs-379585/v1>

**License:**  This work is licensed under a Creative Commons Attribution 4.0 International License.

[Read Full License](#)

---

# **The Effects of Additional Two Bendings on Manufacturing Thin-walled Tube made of AZ31 Magnesium Alloy Fabricated by New Compound Extrusion**

Xing lin Li, Hongjun Hu\*, Gang Hu, Ou Zhang

Chongqing University of Technology, Chongqing, China, 400050;

\* Corresponding authors. E-mail: hhj@cqut.edu.cn (Hongjun Hu)

**Abstract:** To explore the effects of process parameters on evolution of extrusion forces and temperatures and strains and microstructures for composite extrusion of magnesium alloy tube which includes initial direct extrusion and some steps bending processes subsequently, which is shorten for “TEB” in this paper. The TEB process has been researched by using finite element modeling (FEM) method. The rules of extrusion temperatures and the extrusion forces varying with process parameters have been developed. A TEB process with installed container and die has been constructed to perform tests in order to validate the FEM model with different process conditions. And the microstructures evolution have been researched based on effective strains development. The results showed that refined and uniform microstructures can be achieved by TEB process. The research results showed that the process would produce the serve plastic deformation and improve the recrystallization of the grains. The comparison of FEM simulation and experimental results have been made to obtain the relative important principles of TEB process.

**Keywords:** Magnesium Alloy, FEM, Grains refinement, Dynamic recrystallization

## 1 Introduction

Magnesium alloys were developed primarily as direct replacements for existing aluminum alloys to reduce the weight of aircraft and aerospace structures<sup>[1-2]</sup>. It has been realized that the most efficient way of doing this is to develop low density materials, since weight reduction through reduced component size would lead to low stiffness parts and reduced fatigue life. Typical components that benefit from low density alloys include structural members in air frames, aerospace vehicle skins, and liquid oxygen and hydrogen fuel tanks in spacecraft<sup>[3-4]</sup>.

In recent years, severe plastic deformation (SPD) methods such as equal channel angular extrusion (ECAE) which processed bulk nano-structure materials have attracted the growing interest of specialists in materials science. One phenomenon observed in the case of AZ31 magnesium alloys are the DRX (Dynamic recrystallization) and DRV (Dynamic recovery), which could improve the work ability of the material at elevated<sup>[5-7]</sup>. But the ECAP process is only used in the laboratory scale processing and preparation for nanocrystalline material, there exists an unbridgeable gap between the experiments and industrial applications. The productivity of ECAP in industrial manufacturing is very low, ECAP usually involves a large number of steps and is not easily applied from the laboratory to an industry for it is not a continuous process, but the dimension of extruded rod is the same as the initial billet. Although it has been invented in the early 1980s, the process did not progress as much as one would desire and is still confined to the laboratory scale experiments<sup>[8-10]</sup>.

Composite extrusion method for AZ31 magnesium alloy have been presented which combines the traditional direct extrusion and the severe plastic deformation ECAP (equal channel angular pressing), that is to say extrusion and bending (one or more than one) are combined. To

obtain the deformation mechanisms of a new composite extrusion for thin-walled tube fabricated by extrusion-bending process has been researched which is shorten as “TEB” in this paper.

The TEB as a continuous extrusion processes may improve the industrialization preparation and processing of tubes. In order to secure a process with a sustainable high level of accuracy, tools must be adjusted and utilized precisely. In addition, process parameters must be checked carefully to ensure a high level of quality in production.

Commercial software DEFORM-3D can be used to assist analysis of TEB process. It is accepted that material properties are closely correlated to the microstructures. Process conditions include some extrusion parameters such as the extrusion speeds, the initial temperatures, and friction and heat transfer coefficients of the billets, container and die and have great effects on the microstructures<sup>[11-12]</sup>.

To illustrate the potential industrial application of the TEB process, TEB die used in the extruder has been designed, and TEB process has been simulated. The aim of the present study is to reveal the microstructure evolution and clarify the grain refinements mechanism in AZ31 magnesium alloy during TEB process. The present study employs DEFORM<sup>TM</sup>-3D finite element software to simulate the loads, temperatures and strain evolution during TEB process. The microstructures of AZ31 magnesium alloy sampled from the extrudes tubes have been observed. Deformed microstructures evolution for AZ31 magnesium alloy have been studied in order to analyze the deformation mechanisms of TEB process.

## **2. Simulation and experimental conditions of TEB process**

### **2.1 Material models for AZ31 magnesium alloy**

A thermo-viscoplastic material models have been used for the billet, and thermo-rigid material for the TEB dies have been applied. The flow stress–strain data of the AZ31 magnesium alloy were determined through hot compression tests using Gleeble1500D machine. A set of flow stress–strain curves include the experimental data over a temperature range of 250–550°C and a strain rate range of 0.01-10s<sup>-1</sup> have been used. The flow stress data have been implemented in the commercial FE code DEFORM<sup>TM</sup>. The dislocation density is treated as an internal state variable and it is computed by numerical integration of the evolution equation <sup>[13-15]</sup>.

### **2.2 Simulation conditions**

The description of the physical model includes the material properties of the billet, the forming temperatures, and the friction coefficients between the concave die and the workpiece, punch and die. AZ31 magnesium alloy have been used in the simulation and extrusion experiments. The extrusion tooling consisting of die, container and ram have been made of the H13 hot-work tool steel. The physical properties of AZ31 magnesium alloy are given in Table.1. Schematic of TEB process is shown in Fig.1. Extrusion equipment and extrusion die and mandrel and extruded tube are shown in Fig.2.

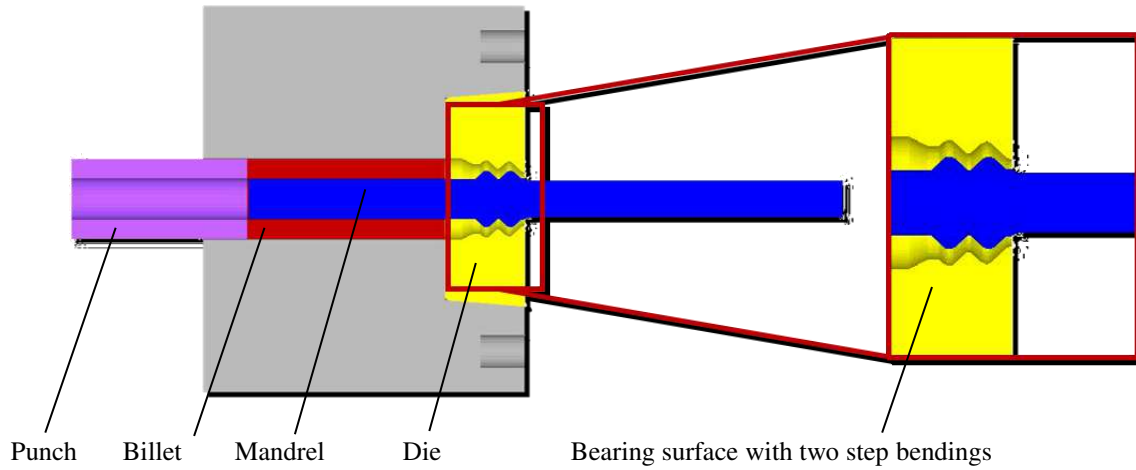


Fig 1. Schematic of TEB process



(a)

(b)

(c)

(d)

Fig. 2. Extrusion equipment (a) and extrusion die (b) and mandrel(c) and extruded tube (d)

The billets and the dies of experiments have identical geometrical parameters and materials with those in simulations. The AZ31 magnesium alloy should be preheated, the ram and the lubricated dies in the furnace have been heated for 2 hours before the actual TEB process. The TEB process is then employed to manufacture the AZ31 magnesium alloy tubes. Real extrusion experiments have been carried out by employing a 200 ton press with a resistance heated container and heaters which are shown in Fig.2b. The die material, die dimensions, billet

dimensions and extrusion conditions are all the same as those used in numerical simulation as described in [Table 2](#). The physical property of AZ31 magnesium alloy is given in [Table1](#). Simulation and experimental parameters are shown in [Table 2](#).

Table 1 Physical properties of AZ31 magnesium alloy <sup>[16-18]</sup>

Property	AZ31 magnesium alloy
Poisson's Ratio	0.35
Coefficient of linear expansion (/°C)	26.8E-6
Density (kg/m <sup>3</sup> )	1780
Poisson's ratio	0.35
Young's modulus (Mpa)	45000
Emissivity	0.12

Table 2 Simulation and experimental parameters

Billet length (mm)	55
Billet outer diameter	39.6
Internal diameter of billet	20.4
Extrusion cylinder diameter	40
extrusion ratio	9.33
Thermal conductivity between billet and die (N/°C. S . mm <sup>2</sup> )	11
Total number of grid elements	32000
Minimum size of grid	1.27
Relative penetration depth	0.7

Grid density type	opposite
Simulation type	Lagrangian incremental
Solver	Conjugate gradient with direct iteration

### **2.3 Experimental setup and tests**

The billets and the container are heated to working temperature by resistance heated device. Billet preheated temperatures of 400°C have been used. The initial temperatures of container and die as well as the ram were 400°C. To preserve the achieved microstructures of the tube after extrusion, the samples have been water quenched for a handling time of 3s. Subsequently, some specimens have been taken from different position in the extruded tube. Microstructures in the as-received, and materials of TEB-received tube are examined by standard metallographic procedures.

## **3. Results and discussion**

### **3.1 Temperature evolution**

During the TEB process, temperature field is affected by many parameters which include initial billet temperatures, TEB speeds, extrusion ratios, and friction coefficients between the billet/die. Even the extrusion of simple rods is a complex process involving highly inhomogeneous deformation and high strain rates. The heat generated by the plastic deformation and friction would increase the temperature of the tubes significantly, and in turn affect the microstructures and mechanical properties. Because TEB process is a non-linear process involving high inhomogeneous deformation and high strain rates, it is difficult to predict the temperatures of

billet accurately<sup>[18,19]</sup>. The average instantaneous temperature of the deforming material at the interface is given by equations (1)<sup>[16]</sup>.

$$T = T_1 + (T_0 - T_1) \exp\left(\frac{-ht}{\rho c \delta}\right) \quad (1)$$

Where  $T_0$  is average temperature of the workpiece,  $T_1$  is average temperature of the die,  $h$  heat transfer coefficient between the material and the dies,  $\delta$  material thickness between the dies. If the temperature increase due to deformation and friction, the final average material temperature  $T_m$  at a time  $t$  is as equations (2)<sup>[17-20]</sup>.

$$T_m = T_d + T_f + T \quad (2)$$

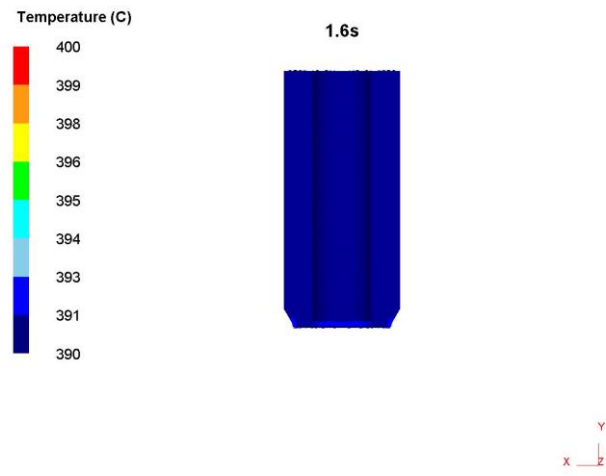
Where  $T_d$  is temperature for frictionless deformation process,  $T_f$  temperature rise due to friction. According to energy conservation principle mathematical models of temperature rise as equations (3) has been established in the TEB deformation zone<sup>[21]</sup>.

$$\Delta T = \frac{(0.29f + 0.9\varepsilon)\sigma_s}{C\rho + h} \quad (3)$$

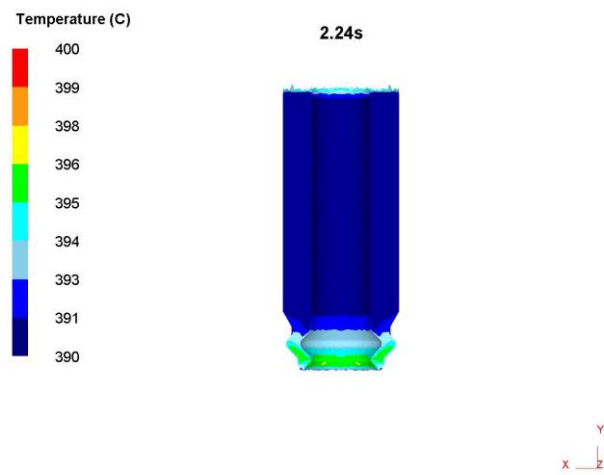
Where  $\Delta T$  is rising temperature, and  $f$  is friction coefficient,  $\varepsilon$  is cumulative strain of plastic deformation,  $C$  is specific heat,  $\rho$  is density,  $h$  is coefficient of heat transfer.

TEB process is divided into multistage according to material flow. Firstly, the tube billet is compressed, and initial tube billet is compressed into the die entrance. Secondly, the extruded tube is formed. Thirdly, the formed tubes are bent consecutively. There is no literature reported to predict the flow patterns of TEB process. Slip-line fields or upper bound approaches have been utilized to predict the flow patterns. But a constant value for the flow stress is assumed by the upper bound approach. The problem can be solved by numerical simulation with the development of three-dimensional FEM. In this study, the material flow during the extrusion process is

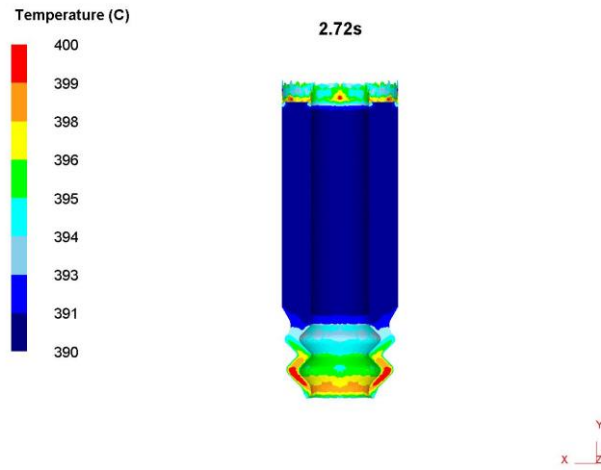
demonstrated clearly by simulation.



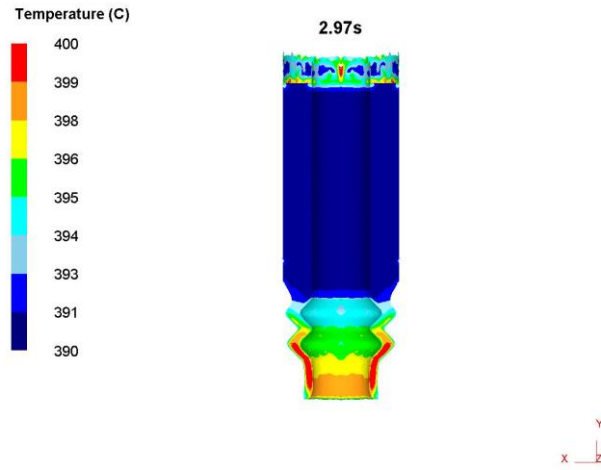
(a)



(b)



(c)



(d)

Fig.3. Temperature contours in the billet extruded at a ram speed of 20 mm/s and at the displacements of: (a)  $t = 1.6$  s, (b)  $t = 2.24$  s, (c)  $t = 2.72$ s, (d)  $t = 2.97$ s.

Fig.3 shows the temperature contours in the extruded tube at the extrusion time of 1.6 s, 2.24 s, 2.72s and 2.97s corresponding to direction extrusion stage and the bending stages of the process, respectively. Comparison of the temperature distributions at these two positions demonstrates the thermal characteristics within the billet, and the heat transfer from the deformation zone in front

of the die towards the outsides of the tube billet. Fig.3a shows that the temperatures of the tube billets at the beginning of the process are various and below the initial billet temperature 400°C if heat is produced in the extrusion zone and temperature gradients are formed. Obviously, this is due to heat loss to the TEB die. The heat flow along the radial direction and the axial direction in the tube billet. It is apparent that heat has already been conducted toward the periphery and the rear end of the billet. Temperatures for about a half of the billet below the initial billet temperature in Fig.3b, the reason is the result of time available for continuous heat loss to the TEB die and through the die the ambient surround.

The temperature evolution in the billet (initial temperature 400°C) as the TEB process proceeds steady state is shown in Fig.3. It is clear that temperatures of rod surface decrease continuously with development of TEB process. The factors to decrease temperature during the TEB process are (1) heat transfer from die and punch, (2) frictions between the rod material and die, and (3) plastic deformation during the TEB process <sup>[22]</sup>.

It is noticed that the difference increases of maximum temperature predicted by the finite element simulations are not significant. It is uniquely founded that the decrease of the maximum temperature is not change significantly. The reason for the temperature reduction is mainly due to temperature gradient between the die and tube billets. Since the temperature rise depends on the heat generation within the deformation zone. Heat generation depends on the internal power of deformation and frictional power. Variations of different parameters affect the power constituents which affects the heat generation within the deformation zone. Bigger surface temperatures may cause surface cracks and tears for the tensile strength of the AZ31 magnesium alloy.

### 3.2. Load–stroke curve of TEB process

TEB process is a hot working process, the AZ31 magnesium alloy may be heated over recrystallization temperature to keep the material from work hardening and make it easier to push the material through the die. TEB process could be done on hydraulic presses that range from 100 to 11,000 metric tons. As a result of FE analysis, Fig.4 shows load–stroke for TEB process which have been obtained from the finite element simulations with initial temperature of 400 °C.

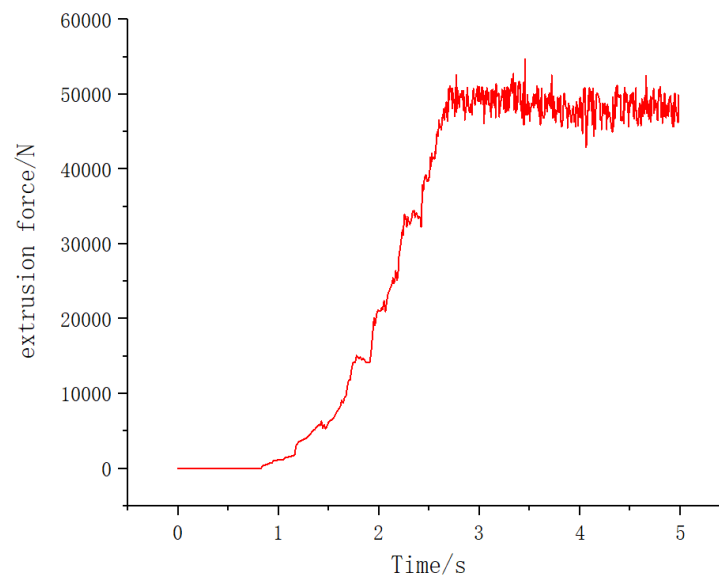


Fig.4. Curve of load-stroke during TEB process

The values for maximum extrusion forces are obtained from the finite element simulation by high-resolution history plots. The extrusion load curve can be divided into three stages: the extrusion upsetting stage and the direction extrusion stage and continuous shears. At the initial stage, the load increases slowly during upsetting phase. When contacting with die channels, the tube is subjected to severe plastic deformation. The load increased rapidly to the first maximum load and the value is about 1 ton, the force of this stage is not steady. But the load increases rapidly due to the work hardening which result from the continuous accumulation of dislocations

and the values of extrusion forces are almost equivalent. The Increments of force become slowly after 2.5 s, and TEB process is in the steady-stage, and the values of extrusion forces are varying periodically. The load-stroke curves could exhibit the characteristic of strain softening with a peak stress to a steady state regime, which is a typical phenomenon caused by the dynamic recovery or recrystallization.

### **3.3. Strain convolutions of TEB process**

Strain is a measure of the degree of deformation in an object. A detailed description of strain is available in any standard text on mechanics of materials, metal forming analysis, or plasticity. The distributions of strain rate in Fig.5 show that the strain distribution is relatively steady throughout the whole extrusion cycle from the direct extrusion to the multi-step bending deformation. In order to gain the deformation characteristics of tube billets for TEB process, the predicted effective strains provide quantitative insight into the deformation behaviors of tube billet during TEB process. Figures in Fig.5 show the effective strain contours of tube billets, which provided the important information regarding the effective strains distribution. The strain distributions for deformation ways of billets are significantly different. The Fig.5a shows the strain distributions for direct extrusion when extrusion times are 1.67s, and strain distribution is characterized by symmetry along the extrusion axis.

Strain - Effective (mm/mm)

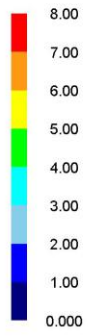


1.67s

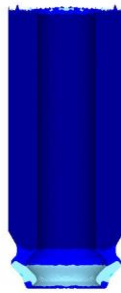


(a)

Strain - Effective (mm/mm)

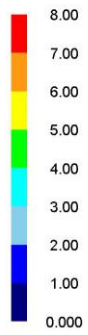


2.23s



(b)

Strain - Effective (mm/mm)



2.68s



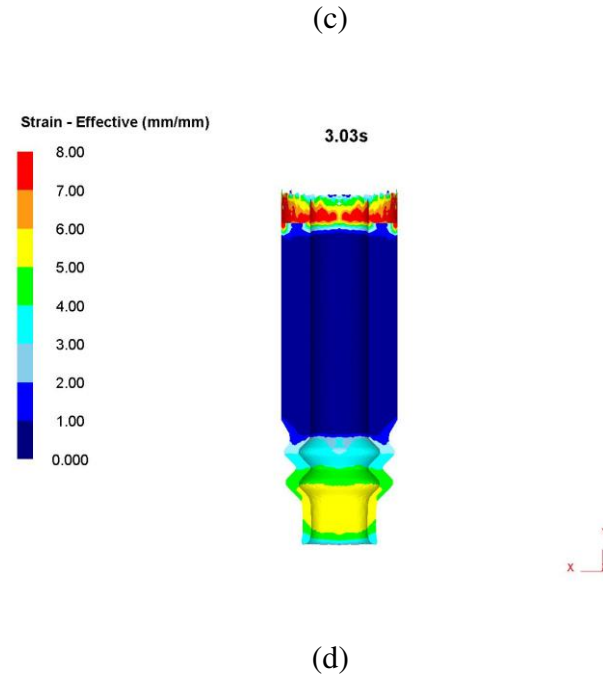


Fig.5. Evolution of strains at different extrusion time during extrusion at a ram speed of 20 mm/s.  
 (a)  $t = 1.67$  s, (b)  $t = 2.23$  s, (c)  $t = 2.68$ , (d)  $t = 3.03$  s.

Distributions of the strain are lamellar with distinct deformation gradients after the first bend of TEB process in the Fig.5b. The deformation of this zone is close to the simple shear deformation in the extrusion time 1 s. The maximum strain increase from 2 to 3. From the strain evolution during the TEB process it can be found that the strains increase with the TEB process progressing, the reason is that the dynamic recrystallizations take place.

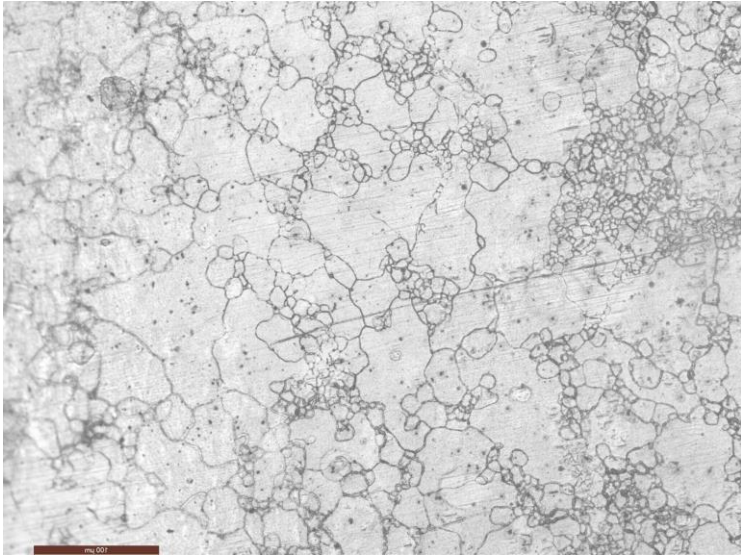
Fig.5c and Fig.5d indicate the strain distributions when extrusion time are 2.68 s and 3.03 s respectively. It can be found that the minimum and maximum strains are respectively by comparing with the values caused by direct extrusion in the Fig.5a and Fig.5b, and the effective strains increase obviously. It indicates that the largest strains exist in the corner region, where the simple shearing occurs. The TEB process would increase the cumulative strain enormously by

comparing with the direct extrusion. The serve plastic deformation can be obtained by additional two bendings. The distribution patterns are very similar in spite of the fact that the actual values are somewhat different.

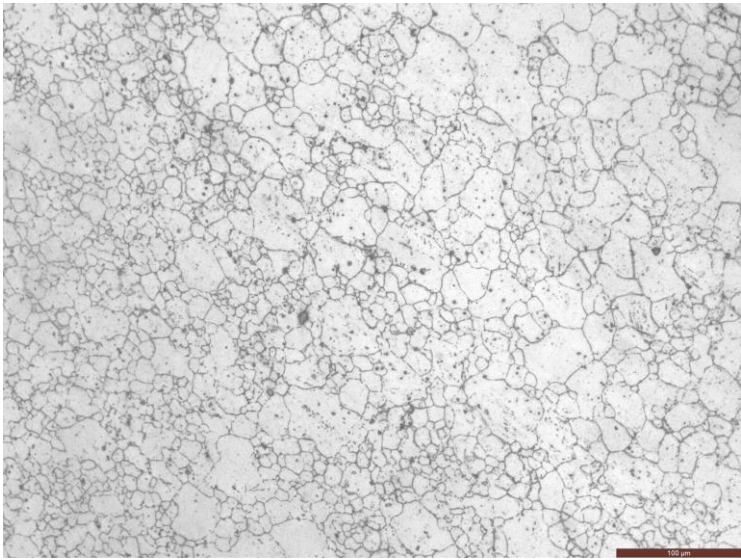
The principle of TEB process is to introduce compressive and accumulated shear strains into the samples. The characters of TEB process are that the sample is subjected to two bendings. Accumulative strain is introduced by reduction in the cross sectional area. ECAE produces significant deformation strain without reducing the cross sectional area. This is accomplished by extruding the workpiece around two corners. The accumulative strains of TEB process can be expressed as equations (5) which include accumulative strain of direct extrusion and two continuous bendings[23]. The TEB dies are completely filled in the case of perfectly plastic material. The multiple bendings of the TEB process produce a systematic increase of deformation, leading to a successive decrease in grain size by means of forming a grid of first low-angle and then high-angle boundaries. Maximum strains in the whole workpiece are seen in the plastic deformation zone.

### **3.4 Microstructures observation**

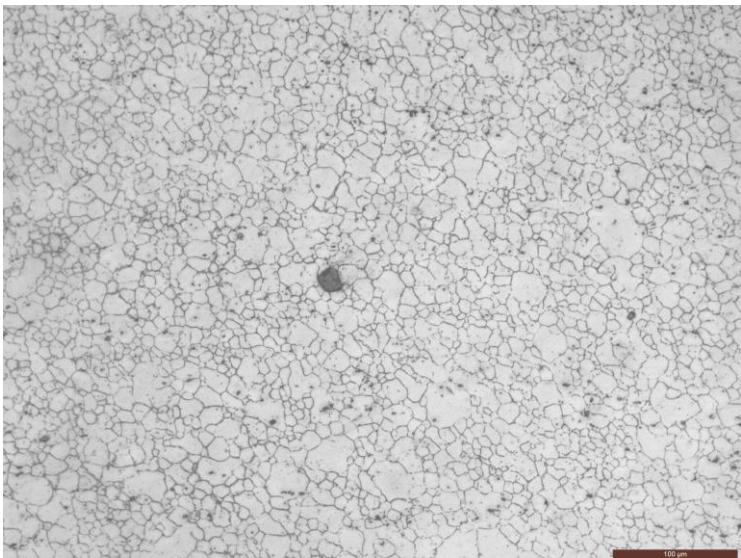
Fig.6 shows the microstructures in three parts within formed tube prepared by TEB process.. The use of TEB process, the average grain size can be changed from 100 $\mu\text{m}$  to 10 $\mu\text{m}$ ; the microstructures were not only clearly refined but also relatively uniform. This is because the TEB process includes additional two bendings. So that the deformation degree of central part of rods increased, the part recrystallization occurred. Therefore, the microstructures became smaller and more homogeneous.



(a)



(b)



(c)

Fig.6 Microstructures of deformed specimens of AZ31 magnesium alloy in different part of TEB die,(a) $t=0.653$  s, (b)  $t=1$  s, (c)  $t=3.32$  s.

The relationship between the average recrystallization grain size ( $d$ ) and the Zener-Hollomon parameter ( $Z$ ) during dynamic recrystallization is given by equation (4).

$$-\ln d = A + B \ln Z \quad (4)$$

Where  $\dot{\epsilon}$  is strain rate,  $Q$  is the activation energy for the deformation,  $T$  is the temperature and  $R$  is the gas constant,  $A$  and  $B$  are constant.

Dynamic recrystallization (DRX) is one of the interesting mechanisms of microstructure evolution. Grain refinement could be attributed to continuous dynamic recrystallization which involves a progressive increase in grain boundary disorientation and changes of low angle boundaries into high angle boundaries. The Zener-Hollomon parameter ( $Z$ ) of first direct extrusion is equal to  $Z_1$ ,  $v_1$  is the extrusion speed.  $\lambda$  is the extrusion ratio,  $R_1$  is the billet radius.

$$Z_1 = \frac{3v_1}{R_1} \ln \lambda \exp\left(\frac{Q}{RT}\right) \quad (5)$$

And the  $Z$  parameters of first and second shearing are  $Z_2$ ,  $Z_3$  respectively.

$$Z_2 = Z_3 = \left[ \frac{2 \cot\left(\frac{\phi}{2} + \frac{\psi}{2}\right) + \psi \csc\left(\frac{\phi}{2} + \frac{\psi}{2}\right)}{\sqrt{6}} \right] \frac{\sqrt{v_2}}{\psi R_2} \exp\left(\frac{Q}{RT}\right) \quad (6)$$

Where inner corner angle ( $\Phi$ ), outer corner angle ( $\psi$ ).  $V_1$  is the speed of extruded rods.  $R_2$  is radius of extruded rod.

Based on the present TEB process with extrusion temperature  $400^\circ\text{C}$ , from the equation(4) to equation(6) it can be found that the accumulative strain increase with the extrusion advancing, so the grains will be refined consequently. It is clear that there are four phases recrystallization during TEB process. It can be found that the average sizes of grains for DRX were coarsened with the preheating temperature rise and  $Z$  parameter decreases with the temperatures.

## **4. Conclusions**

Three-dimensional finite element DEFORM software has been utilized to research the plastic deformation behavior of AZ31 magnesium alloy tube during TEB process through a TEB combination die. The evolution of extrusion loads curves and effective stresses and temperatures can be divided into two stages including direction extrusion stage and multi-bendings. Through the combination of finite element models and experiments, the high temperature region in the experimental process is mainly in the deformation zone, and different friction factors would affect the stresses and strains in the billets, and the tube can be obtained easier under the smaller friction factors. The effects of different temperatures on stress distributions are as follows: the temperature is higher, and the stress distribution in the billet is smaller, but too high temperature would lead to the coarse grain sizes and decrease the mechanical properties of the finished tubes. The deformation degree and uniformity of microstructures for the tube can be controlled by the preheated temperatures and extrusion speeds of TEB process. The strengths and accuracies of tube and grain refinements could be controlled. TEB-extruded AZ31 magnesium alloy sample could produce fine-grained microstructures for TEB process would cause severe plastic deformation and improve the dynamic recrystallization during TEB process. Zener-Hollomon parameters during TEB process showed that the grains of AZ31 magnesium alloy would be refined gradually. The large strain rates can be introduced into the extrusion and continuous multi-bending deformation, which would promote the occurrence of dynamic recrystallization of AZ31 magnesium alloy, at the same time reduce or eliminate the defects in the interior of the microstructures.

## **Funding information**

This work was supported by the National Science Foundation of China (52071042, 51771038 and 51571040), and Chongqing talent plan (CQYC202003047), and Chongqing Natural Science Foundation Project of cstc2018jcyjAX0249 and cstc2018jcyjAX0653 ).

## **DECLARATIONS**

### **-Ethical Approval**

No animals have been used in any experiments.

### **-Consent to Participate**

There are no human who have been used in any experiments.

### **Consent to Publish**

The Author confirms:

- that the work described has not been published before (except in the form of an abstract or as part of a published lecture, review, or thesis);
- that it is not under consideration for publication elsewhere;
- that its publication has been approved by all co-authors, if any;
- that its publication has been approved (tacitly or explicitly) by the responsible authorities at the institution where the work is carried out.

The Author agrees to publication in the Journal indicated below and also to publication of the article in English by Springer in Springer's corresponding English-language journal.

The copyright to the English-language article is transferred to Springer effective if and when the

article is accepted for publication. The author warrants that his/her contribution is original and that he/she has full power to make this grant. The author signs for and accepts responsibility for releasing this material on behalf of any and all co-authors. The copyright transfer covers the exclusive right to reproduce and distribute the article, including reprints, translations, photographic reproductions, microform, electronic form (offline, online) or any other reproductions of similar nature.

After submission of the agreement signed by the corresponding author, changes of authorship or in the order of the authors listed will not be accepted by Springer.

Journal:

Title in English :The International Journal of Advanced Manufacturing Technology

Title of article: The Effects of Additional Two Bendings on Manufacturing Thin-walled Tube made of AZ31

Magnesium Alloy Fabricated by New Compound Extrusion

Names of ALL contributing authors: Xin lin Li,Hongjun Hu,Gang Hu,Ou Zhang

Corresponding author's signature:

Hu H-J

Date: 2021-04-01

### **-Authors Contributions**

- Xing lin Li done the experoments.
- Hongjun Hu is corresponding author of this paper who wrote the paper.
- Gang Hu done the examples in this paper.
- Ou Zhang researched the microstructures analysises in this paper.

### **-Funding**

This work was supported by the National Science Foundation of China (52071042, 51771038 and 51571040), and Chongqing Natural Science Foundation Project of cstc2018jcyjAX0249 and cstc2018jcyjAX0653 andcstc2016jcyjA0434, and Scientific and Technological Research Program of Chongqing Municipal Education Commission (KJ1600924), and Science and Technology Planning in Banan District of Chongqing City (No.0109184334).

I confirm that I have mentioned all organizations that funded my research in the

Acknowledgements section of my submission, including grant numbers where appropriate.

## **Competing Interests**

The authors declare no competing non-financial/financial interests.

## **-Availability of data and materials**

The raw/processed data required to reproduce these findings cannot be shared at this time as the data also forms part of an ongoing study.

## **References**

[1]Lv J, Liang T, Wang C, et al. The passive film characteristics of several plastic deformation 2099 Al–Li alloy[J]. Journal of Alloys & Compounds, 2016, 662:143-149.

[2]Koralnik M, Adamczyk-Cieślak B, Mizera J. The influence of the complex deformation on the

- microstructure and mechanical properties of the model Al-Li alloys[J]. 2016(5-6):508-509.
- [3]Ma Y, Zhou X, Liao Y, et al. Localised corrosion in AA 2099-T83 aluminium-lithium alloy: The role of grain orientation[J]. Corrosion Science, 2016, 107:41-48.
- [4]Zhang F, Sun J L, Shen J, et al. Flow behavior and processing maps of 2099 alloy[J]. Materials Science & Engineering A, 2014, 613(613):141-147.
- [5] A. Bois-Brochu, C. Blais, F.A.T. Goma, D. Larouche, J. Boselli, M. Brochu, Characterization of Al-Li 2099 extrusions and the influence of fiber texture on the anisotropy of static mechanical properties, Materials Science and Engineering: A, 597(2014) 62-69.
- [6] Y. Prasad, H.L. Gegel, S.M. Doraivelu, J.C. Malas, J.T. Morgan, K.A. Lark, D.R. Barker, Modeling of Dynamic Material Behavior in Hot Deformation - Forging of Ti-6242, METALLURGICAL TRANSACTIONS A-PHYSICAL METALLURGY AND MATERIALS SCIENCE, 15(1984) 1883-1892.
- [7] Y.V.R.K. Prasad, T. Seshacharyulu, Processing maps for hot working of titanium alloys, Materials Science and Engineering: A, 243(1998) 82-88.
- [8] S.V.S. Narayana Murty, B. Nageswara Rao, B.P. Kashyap, Identification of flow instabilities in the processing maps of AISI 304 stainless steel, J MATER PROCESS TECH, 166(2005) 268-278.
- [9] L. Qing, H. Xiaoxu, Y. Mei, Y. Jinfeng, On deformation-induced continuous recrystallization in a superplastic Al-Li-Cu-Mg-Zr alloy, Acta Metallurgica et Materialia, 40(1992) 1753-1762.
- [10]S. Kobayashi, T. Yoshimura, S. Tsunekawa, T. Watanabe, J. Cui, Grain Boundary Microstructure-Controlled Superplasticity in Al-Li-Cu-Mg-Zr Alloy, (2003).

- [11] A. Ma, F. Roters, A constitutive model for fcc single crystals based on dislocation densities and its application to uniaxial compression of aluminium single crystals, *ACTA MATER*, 52(2004) 3603-3612.
- [12] H. Garmestani, S. Lin, B.L. Adams, S. Ahzi, Statistical continuum theory for large plastic deformation of polycrystalline materials, *J MECH PHYS SOLIDS*, 49(2001) 589-607.
- [13] M.H. F. J. Humphreys. *Recrystallization and Related Annealing Phenomena*, Second Edition (Pergamon Materials Series), Pergamon, 2004.
- [14] Z. Sun, L. Zheng, H. Yang, Softening mechanism and microstructure evolution of as-extruded 7075 aluminum alloy during hot deformation, *MATER CHARACTER*, 90(2014) 71-80.
- [15] H.J. McQueen, Examining the Mechanisms of Dynamic Recrystallization (DRX) in two-phase Al alloys, *PROCEEDINGS OF THE 13TH INTERNATIONAL CONFERENCE ON ALUMINUM ALLOYS (ICAA13)*, (2012) 1761-1766.
- [16] H.J. McQueen, W. Blum, Dynamic recovery: sufficient mechanism in the hot deformation of Al (< 99.99), *Materials Science and Engineering: A*, 290(2000) 95-107.
- [17] H.J. McQueen, Development of dynamic recrystallization theory, *Materials Science and Engineering: A*, 387-389(2004) 203-208.
- [18] E. Nes. *Superplastic* (edited by B. Baudelet and M. Suery), Editions du C.N.R.S, Paris, 1985.
- [19] G. Winther, X. Huang, N. Hansen, Crystallographic and macroscopic orientation of planar dislocation boundaries - Correlation with grain orientation, *ACTA MATER*, 48(2000) 2187-2198.
- [20] X. Huang, Grain Orientation Effect on Microstructure in Tensile Strained Copper, *SCRIPTA MATER*, 38(1998) 1697-1703.
- [21] N. Hansen, D.J. Jensen, Development of microstructure in FCC metals during cold work,

PHILOS T R SOC A, 357(1999) 1447-1469.

[22]X. Yu, Y. Zhang, D. Yin, Z. Yu, S. Li, Characterization of Hot Deformation Behavior of a Novel Al–Cu–Li Alloy Using Processing Maps, *Acta Metallurgica Sinica (English Letters)*, 28(2015) 817-825.

[23]H. Yin, H. Li, X. Su, D. Huang, Processing maps and microstructural evolution of isothermal compressed Al–Cu–Li alloy, *Materials Science and Engineering: A*, 586(2013) 115-122.

# Figures

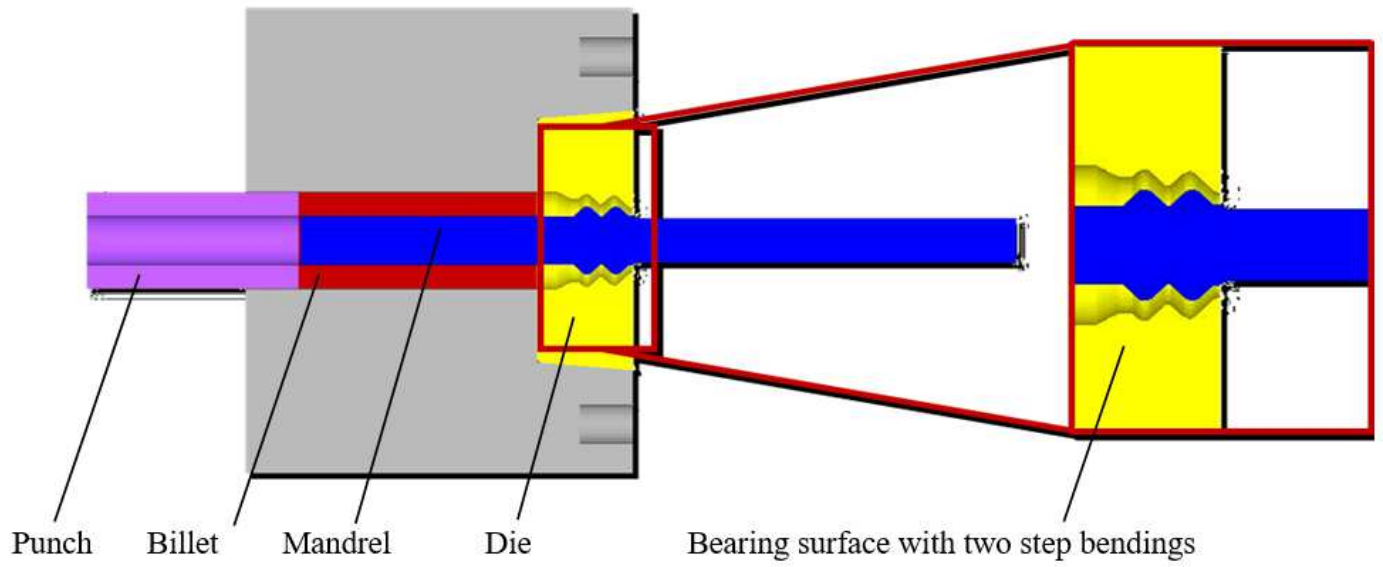


Figure 1

Schematic of TEB process

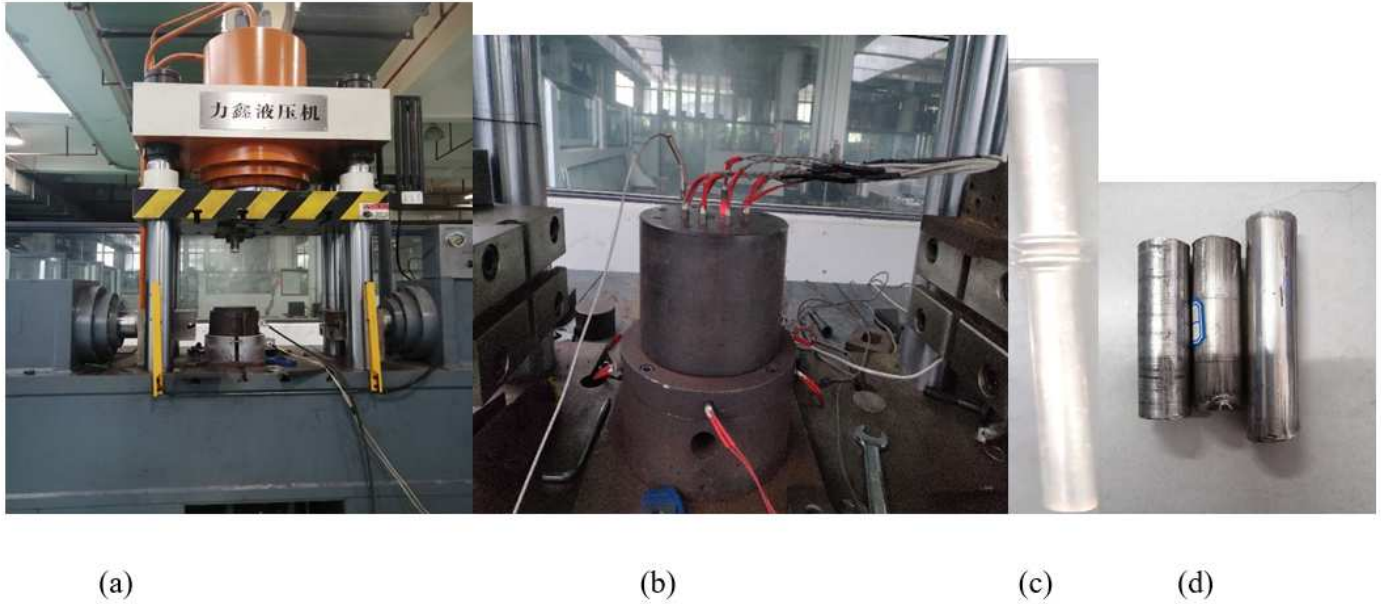
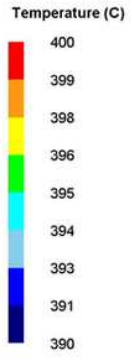
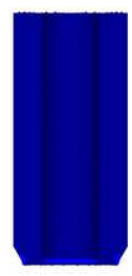


Figure 2

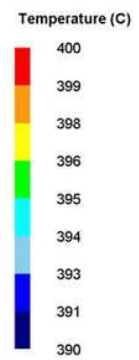
Extrusion equipment (a) and extrusion die (b) and mandrel(c) and extruded tube (d)



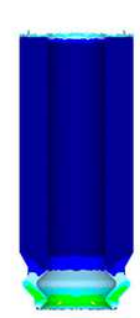
1.6s



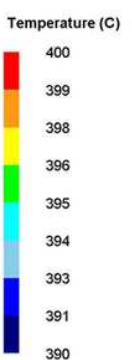
(a)



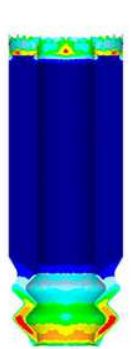
2.24s



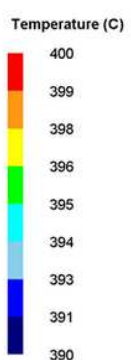
(b)



2.72s



(c)



2.97s



(d)

**Figure 3**

Temperature contours in the billet extruded at a ram speed of 20 mm/s and at the displacements of: (a)  $t = 1.6$  s, (b)  $t = 2.24$  s, (c)  $t = 2.72$  s, (d)  $t = 2.97$  s.

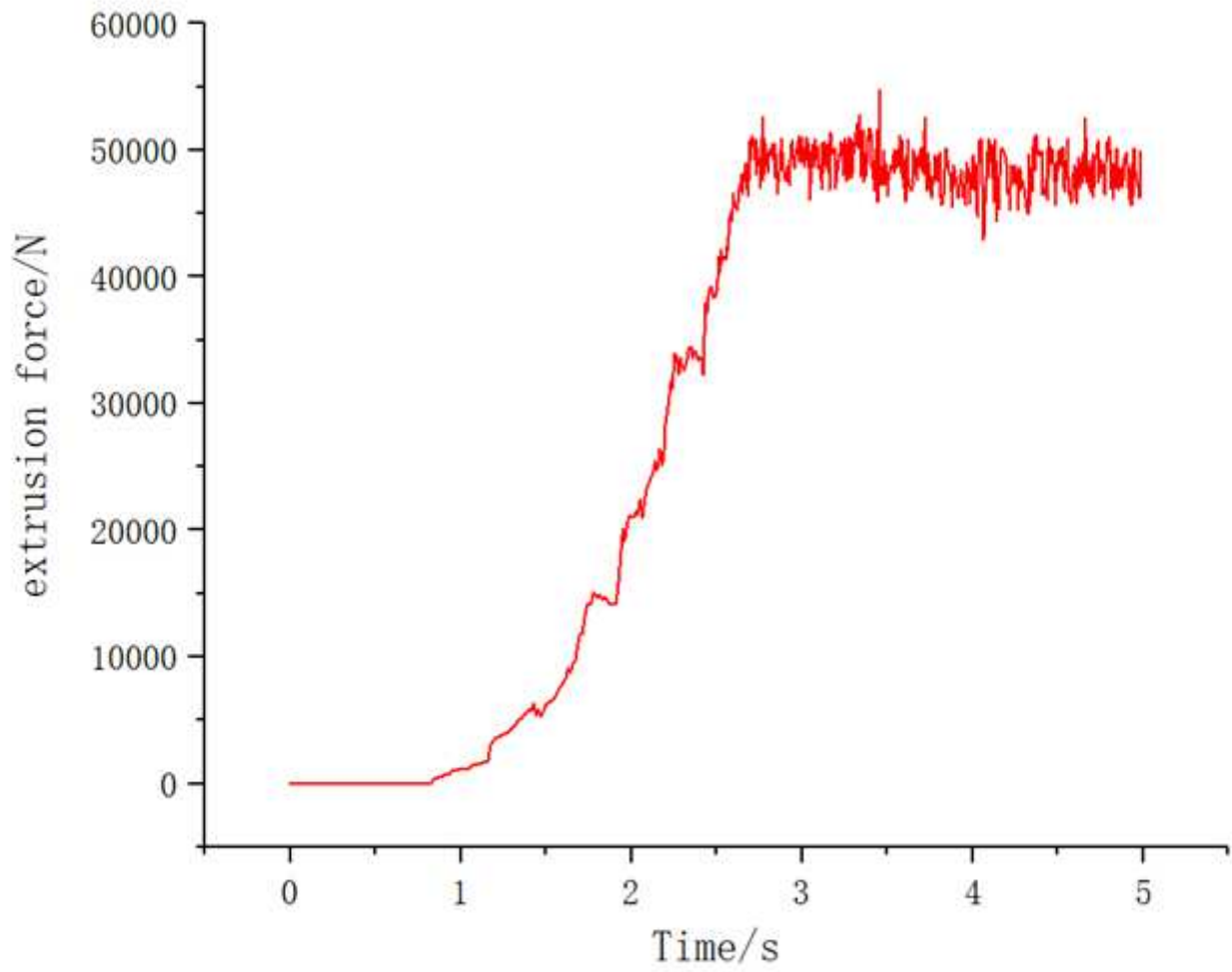


**Figure 4**

Curve of load-stroke during TEB process

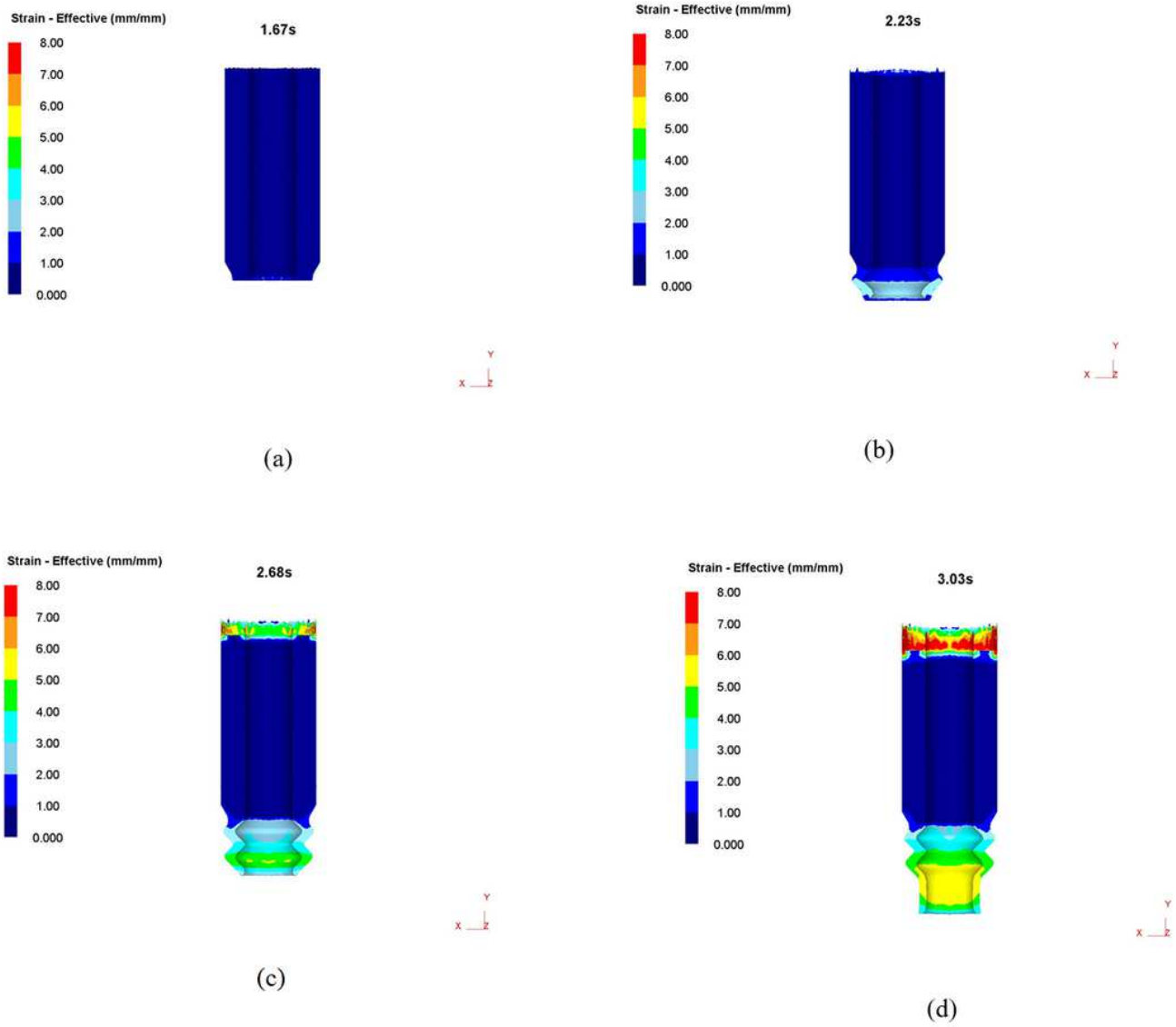
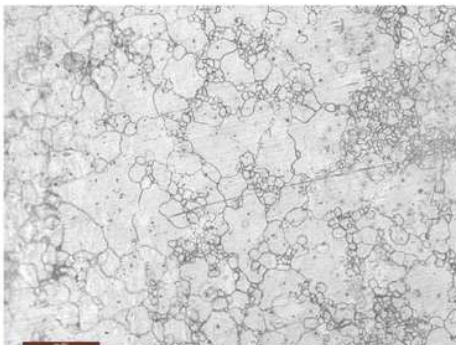
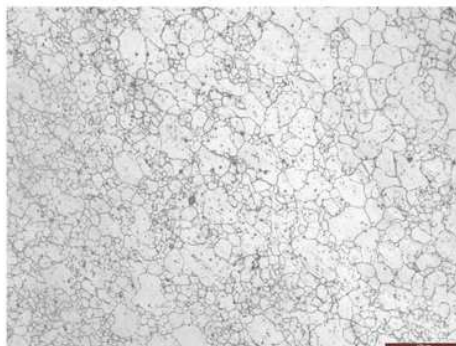


**Figure 5**

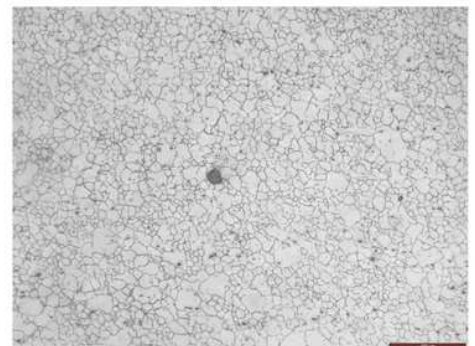
Evolution of strains at different extrusion time during extrusion at a ram speed of 20 mm/s. (a)  $t = 1.67$  s, (b)  $t = 2.23$  s, (c)  $t = 2.68$ , (d)  $t = 3.03$  s.



a



b



c

## Figure 6

Microstructures of deformed specimens of AZ31 magnesium alloy in different part of TEB die, (a)  $t = 0.653$  s, (b)  $t = 1$  s, (c)  $t = 3.32$  s.